Int. J. Heat Mass Transfer. Vol. 11, pp. 1611–1620. Pergamon Press 1968. Printed in Great Britain

NON-GREY RADIATIVE HEAT TRANSFER BETWEEN PARALLEL PLATES†

G. M. SIMMONS‡ and J. H. FERZIGER

Nuclear Engineering Division, Department of Mechanical Engineering, Stanford University, Stanford, California, U.S.A.

(*Received* 28 *September* 1966 *and in revised form* 1 *January* 1968)

Abstract—The case of radiative transfer between parallel plates separated by an absorbing gas with a "picket fence" absorption coefficient is treated by a method due to Siewert and Zweifel. The problem is reduced to a set of integral equations from which numerical solutions are readily obtained. Exact results are compared with the Planck and Rossland approximations as well as a new approximation. The results indicate that the Rosseland approximation is sufficiently accurate for narrow line widths but that its accuracy diminishes for wider lines or bands.

NOMENCLATURE

A, discrete expansion coefficient, equation (9);
B, modified continuum expansion coefficient, equation (10b);
B_ν, Planck distribution;
c, matrix defined by equation (6b);
D, modified discrete expansion coefficient, equation (10b);
d, dimensionless gas thickness;
f, surface emission coefficient;
g, function defined by equation (16);
I, radiation intensity;
k, index for continuum eigenfunctions;
N, normalization constant defined by equation (11d);
P, principal value;
q, heat flux;
T, $\tanh^{-1}$, temperature;
w, weight function matrix defined by equation (8a);
w_i, fraction of the Planck spectrum in the frequency intervals for which $\sigma = \sigma_i$;
X, fundamental solution function defined by equation (8c);
x, dimensionless spatial variable;
x_*, non-grey Milne extrapolation distance, equation (13c);
z, spatial variable.

Greek symbols

α, continuum expansion coefficient, equation (9);
γ, weight function defined by equation (8b);
δ, delta function;
μ, direction cosine of radiative direction vector with z axis;
ν, frequency;
ρ, density;
Σ, cross-section matrix defined by equation (6a);
σ, absorption coefficient;
$\tilde{\sigma}$, Stefan–Boltzmann constant;
Φ, χ, ψ, eigenfunctions defined by [4];
ξ, cross-section ratio defined by equation (6a).

† Work supported in part by NSF Grants GP-1522, GP-3131 and GK-737.

‡ NSF Predoctoral Fellow. Present address: John Jay Hopkins Laboratory of Pure and Applied Science, General Atomic Division of General Dynamics Corporation, Post Office Box 608, San Diego, California, 92112, U.S.A.

Subscripts and superscripts

- G, grey;
- p, Planck;
- r, Rosseland;
- T, transpose matrix;
- w, wall;
- ν, frequency;
- 1, frequency range with higher absorption coefficient;
- 2, frequency range with lower absorption coefficient.

1. INTRODUCTION

A PREVIOUS article [1] illustrated the application to radiative transfer in grey gases of a method which has enjoyed great success in neutron transport theory. In the present article a generalization of this method is applied to non-grey problems. The method again involves the construction of a complete set of eigenfunctions of the homogeneous transport equation in terms of which any other solution may be expanded. Sources and boundary conditions determine the coefficients in the expansion.

It has been shown that the one-dimensional equation of transfer for a non-grey gas in local thermodynamic and radiative equilibrium [2–5] can be solved by the method of singular eigenfunctions provided that the expression

$$\frac{B_\nu(z)}{\int_0^\infty \sigma_\nu B_\nu(z)\,\mathrm{d}\nu} \tag{1}$$

is independent of position, where $B_\nu(z)$ is the Planck distribution function. This is the case for several interesting models of the absorption coefficient, σ_ν [6].

(a) Elsasser model—in this case, σ_ν is assumed to consist of identical equi-spaced lines.
(b) Mayer–Goody model—here σ_ν consists of randomly distributed lines. The lines may be either identical or of random height and width.

The essential property of these models is that, if the line density is high enough, it is possible to divide the frequency range into intervals small enough that the Planck distribution function, $B_\nu(z)$, is essentially constant over each interval but large enough that the average of σ_ν over each interval is constant. Then the desired property mentioned above obtains.

The simplest non-trivial special case of these models is one in which the absorption coefficient, σ_ν, takes on only two discrete values, σ_1 and σ_2, i.e. the "picket fence" model. Thus, we consider a gas with an absorption coefficient consisting of an infinite number of spectral lines superimposed on a uniform grey background. The absorption coefficient of such a gas is depicted in Fig. 1. The (rectangular) spectral lines are assumed to have absorption coefficient σ_1 while the absorption coefficient of the grey background is σ_2 and, in keeping with the above discussion, the fraction of frequencies covered by the lines is assumed to be independent of frequency. Methods of solving radiative transfer problems for the picket fence model were given by Siewert and Zweifel [4]; they have extended their work to the case in which the absorption coefficient takes on N discrete values [5] and it is also possible to extend the method to the continuous case [3, 7]. It should be noted that the picket fence model was also used by Greif [8].

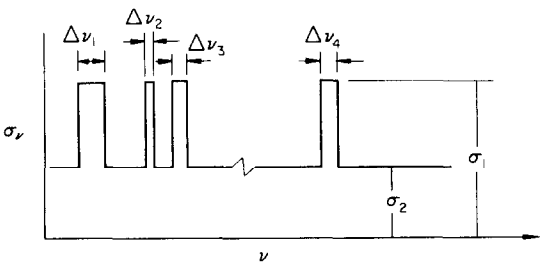

FIG. 1. Frequency dependence of the absorption coefficient in the picket fence model.

In this paper we shall consider energy transfer between parallel plates separated by a picket fence gas and shall ignore conductive and convective transfer. The major objective is to develop an exact calculation of the heat transfer and temperature distribution (in the picket fence

model) and to compare the results with approximate methods in current use, in particular the Rosseland approximation [9]. The primary motive for restriction to this model is that it allows us to take advantage of results presented by Siewert and Zweifel [4], thus reducing the labor considerably.

Although the model used is a crude representation of the absorption coefficient, there is no reason why the approximate methods should be any better or worse for this model than for more exact models. Our calculations should therefore be a reasonable test of the approximate methods.

2. STATEMENT OF THE PROBLEM

For the two-value picket fence model of the absorption coefficient the denominator of expression (1) becomes

$$\int_0^\infty \sigma_\nu B_\nu(z)\,d\nu = \sigma_1 w_1 + \sigma_2 w_2 \tag{2}$$

where w_i is the fraction of the Planck spectrum in the frequency interval for which the absorption coefficient is $\sigma_i (i = 1, 2)$. Under the assumptions of local thermodynamic and radiative equilibrium, the equation of radiative transfer can then be written

$$\frac{\mu}{\rho(z)}\frac{\partial I_\nu}{\partial z} + \sigma_\nu I_\nu(z,\mu) = \frac{\sigma_\nu B_\nu(z)}{2(\sigma_1 w_1 + \sigma_2 w_2)} \times \int_0^\infty \sigma_{\nu'}\,d\nu' \int_{-1}^{1} I_{\nu'}(z,\mu')\,d\mu'. \tag{3}$$

Then, integrating separately over each of the intervals for which σ takes its two possible values, and defining

$$dx = \rho(z)\sigma_2\,dz \tag{4}$$

where it is assumed (as mentioned earlier) that $\sigma_2 < \sigma_1$, we find, in matrix notation,

$$\mu\frac{\partial}{\partial x}\mathbf{I}(z,\mu) + \boldsymbol{\Sigma}\mathbf{I}(x,\mu) = \mathbf{c}\int_{-1}^{1}\mathbf{I}(x,\mu')\,d\mu' \tag{5}$$

where the components of $\mathbf{I}(I_1, I_2)$ represent the total intensity in each of the two frequency intervals and

$$\boldsymbol{\Sigma}_{ij} = \xi_i\delta_{ij} \tag{6a}$$

$$c_{ij} = \frac{\xi_i\xi_j w_i}{2(\xi_1 w_1 + w_2)} \tag{6b}$$

$$\xi_i = \sigma_i/\sigma_2. \tag{6c}$$

Equation (5) is the starting point of the analysis of Siewert and Zweifel [4].

For the problem at hand, we wish to solve equation (5) subject to the boundary conditions

$$\mathbf{I}(-d/2,\mu) = \mathbf{f}(\mu) = \begin{pmatrix} f_1(\mu) \\ f_2(\mu) \end{pmatrix} \qquad \mu > 0 \tag{7a}$$

$$\mathbf{I}(d/2,\mu) = 0 \qquad \mu < 0 \tag{7b}$$

where $f_i(\mu)$ represents the intensity emitted by the left plate in frequency interval i and may be prescribed arbitrarily. The problem in which both plates emit may be solved by superposing the appropriate solutions of the problem under consideration [1].

The method to be used is as follows. A complete set of (singular) elementary eigenfunctions of equation (5) can be constructed [4] using Case's method [10]. The solution to the problem under consideration can then be expanded in terms of these eigenfunctions and the unknown expansion coefficients determined such that the boundary conditions are satisfied.

These functions are complete in the sense that any pair of functions

$$\mathbf{f}(\mu) = \begin{pmatrix} f_1(\mu) \\ f_2(\mu) \end{pmatrix}$$

defined on $-1 \leqslant \mu \leqslant 1$ may be represented as a linear combination of these eigenfunctions (full range completeness). They also have the property that a reduced set of eigenfunctions is complete for functions defined on $0 \leqslant \mu \leqslant 1$ (half range completeness) [4].

The coefficients in the expansions mentioned above are most easily computed by use of

orthogonality relations. For the half-range case a scalar product is defined by

$$[E, G] \equiv \int_0^1 E^T(k', \mu)\, w(\mu)\, G(k, \mu)\, \mathrm{d}\mu$$

where the T denotes transpose. The weight function (matrix) is given by

$$w(\mu) = \begin{pmatrix} \xi_1 \gamma(\mu/\xi_1) & 0 \\ 0 & \gamma(\mu) \end{pmatrix} \tag{8a}$$

where

$$\gamma(\mu) = \frac{3\mu\xi_1}{X(-\mu)} \begin{pmatrix} \dfrac{\xi_1 w_1 + w_2}{\xi_1 w_2 + w_1} \end{pmatrix}. \tag{8b}$$

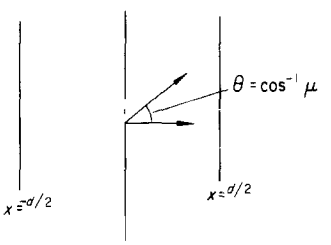

FIG. 2. Coordinate system.

3. SOLUTION OF THE PROBLEM

We wish to solve equation (5) subject to boundary conditions (7). Since equation (5) is homogeneous, we can represent the solution as a linear superposition of the solutions presented in [4].

$$\begin{aligned} \mathbf{I}(x, \mu) = {} & A_+ \boldsymbol{\psi}_+(x, \mu) + A_- \boldsymbol{\psi}_-(x, \mu) \\ & + \int_{①} \alpha_1(k)\, \mathrm{e}^{-x/k}\, \boldsymbol{\Phi}_1(k, \mu)\, \mathrm{d}k \\ & + \int_{①} \alpha_2(k)\, \mathrm{e}^{-x/k}\, \boldsymbol{\Phi}_2^{(1)}(k, \mu)\, \mathrm{d}k \\ & + \int_{②} \alpha_2(k)\, \mathrm{e}^{-x/k}\, \boldsymbol{\Phi}_2^{(2)}(k, \mu)\, \mathrm{d}k \end{aligned} \tag{9}$$

where A_+, A_-, $\alpha_1(k)$ and $\alpha_2(k)$ are unknown expansion coefficients and the subscripts on the integrals denote integration over regions 1 and 2 defined by Siewert and Zweifel [4].

We give only a brief description of the method of solution. Each integral in equation (9) is split into two integrals, one with $k < 0$ and one with $k > 0$. The expansion (9) is then substituted into the boundary conditions (7) and the resulting equations are added and subtracted from each other. There results the pair of singular integral equations:

$$\begin{aligned} \mathbf{f}(\mu) = {} & D_\pm + \int_0^{1/\xi_1} B_{1\pm}(k)\, \boldsymbol{\Phi}_1(k, \mu)\, \mathrm{d}k \\ & \pm \int_0^{1/\xi_1} B_{1\pm}(k)\, \mathrm{e}^{-d/k}\, \boldsymbol{\Phi}_1(-k, \mu)\, \mathrm{d}k \\ & + \int_0^{1/\xi_1} B_{2\pm}(k)\, \boldsymbol{\Phi}_2^{(1)}(k, \mu)\, \mathrm{d}k \\ & \pm \int_0^{1/\xi_1} B_{2\pm}(k)\, \mathrm{e}^{-d/k}\, \boldsymbol{\Phi}_2^{(1)}(-\mathrm{k}, \mu)\, \mathrm{d}k \\ & + \int_{1/\xi_1}^1 B_{2\pm}(k)\, \boldsymbol{\Phi}_2^{(2)}(k, \mu)\, \mathrm{d}k \\ & \pm \int_{1/\xi_1}^1 B_{2\pm}(k)\, \mathrm{e}^{-d/k}\, \boldsymbol{\Phi}_2^{(2)}(-k, \mu)\, \mathrm{d}k \\ & 0 \leqslant \mu \leqslant 1 \end{aligned} \tag{10a}$$

where we have defined

$$\left.\begin{aligned} D_+ &= 2A_+ \boldsymbol{\psi}_+(d/2, \mu) \\ D_- &= -2A_- \boldsymbol{\psi}_-(d/^2, \mu) \\ B_{j\pm}(k) &= [\alpha_j(k) \pm \alpha_j(-k)]\, \mathrm{e}^{d/2k}. \end{aligned}\right\} \tag{10b}$$

Equations (10) can be converted to Fredholm equations by making use of the orthogonality relations presented by Siewert and Zweifel [4], and certain "crossing relations" involving the functions with k replaced by $-k$; note that these are not found in [4]:

$$\begin{aligned} [\boldsymbol{\chi}_2^{(1)}, \boldsymbol{\varphi}_2^{(1)}(-k, \mu)] &= [\boldsymbol{\chi}_2^{(1)}, \boldsymbol{\varphi}_2^{(2)}(-k, \mu)] \\ &= \frac{(c_{11} + c_{22})}{k + k'} kk' X(-k') \end{aligned} \tag{11a}$$

$$[\chi_1^{(1)}, \varphi_2^{(1)}(-k,\mu)] = [\chi_1^{(1)}, \varphi_2^{(2)}(-k,\mu)]$$

$$= \frac{c_{11}c_{21}kk'}{k+k'} X(-k)\{1 + 2kc_{22}[T(\xi_1 k) - T(k)]\} \quad (11b)$$

$$[\chi_1^{(1)}, \psi_-(x,-\mu)] = -\xi_1 c_{11} k\{1 - 2k[T(\xi_1 k) - T(k)]\} \quad (11c)$$

$$[\chi_2^{(1)}, \psi_-(x,-\mu)] = -k(w_2 + \xi_1^2 w_1) \quad (11d)$$

$$[\psi_+, \varphi_2^{(1)}(-k,\mu)] = [\psi_+, \varphi_2^{(2)}(-k,\mu)] = kX(-k) \quad (11e)$$

$$[\varphi_2^{(2)}, \varphi_2^{(2)}(-k,\mu)] = [\varphi_2^{(1)}, \varphi_2^{(1)}(-k,\mu)]$$

$$= [\varphi_2^{(1)}, \varphi_2^{(2)}(-k,\mu)] = \frac{c_{22}kk'}{k+k'} X(-k) \quad (11f)$$

$$[\varphi_1, \varphi_2^{(2)}(-k,\mu)] = [\varphi_1, \psi_-(x,-\mu)] = 0 \quad (11g)$$

$$[\varphi_2^{(1)}, \psi_-(x,-\mu)] = [\varphi_2^{(2)}, \psi_-(x,-\mu)] = -kw_2. \quad (11h)$$

In the derivation of these equations, use has been made of the Poincare–Bertrand formula [11] which governs the interchange of order of integration in principal value integrals. A further discussion of such integrals is given in [12].

Note that the orthogonality relations state that all of the following are zero.

$$\left.\begin{array}{r}[\chi_2^{(1)}, \varphi_1], [\chi_2^{(1)}, \varphi_2^{(2)}], [\chi_2^{(1)}, \psi_\pm], [\chi_1^{(1)}, \varphi_2^{(1)}],\\ [\chi_1^{(1)}, \varphi_2^{(2)}], [\chi_1^{(1)}, \psi_\pm], [\varphi_2^{(2)}, \varphi_2^{(1)}], [\varphi_2^{(2)}, \varphi_1],\\ [\psi_+, \psi_-]\end{array}\right\} \quad (12)$$

Taking the scalar product of equations (14) with the eigenfunction ψ_+ [4] we obtain two equations for the discrete coefficients $A_\pm$:

$$A_+ = \frac{1}{2N_+}\left[[\psi_+, \mathbf{f}] - \int_0^1 B_{2+}(k')\, e^{-d/k'}\, k' X(-k')\, dk'\right] \quad (13a)$$

$$A_- = \frac{-1}{N_+(d + 2x_*)}\left[(\psi_+, \mathbf{f})\right] + \int_0^1 B_{2-}(k')\, e^{-d/k'}\, k' X(-k')\, dk'\Big] \quad (13b)$$

where x_* is the Milne extrapolation length

$$x_* = N_+^{-1}[\psi_+, \psi_-(0,-\mu)]. \quad (13c)$$

Taking the scalar product with $\chi_2^{(1)}$, $\chi_1^{(1)}$ and $\varphi_2^{(2)}$ we obtain three equations for the continuum coefficients.

$$[\chi_2^{(1)}, \mathbf{f}] = D_\pm' + \frac{\gamma(k)}{g_1(k)} B_{2\pm}(k) \pm (c_{11} + c_{22})k \int_0^1 B_{2\pm}(k')\, e^{-d/k'} \frac{k' X(-k')}{k+k'} dk'$$

$$0 \leqslant k \leqslant 1/\xi_1 \quad (14a)$$

$$[\chi_1^{(1)}, \mathbf{f}] = D_\pm'' + \frac{\gamma(k)}{g_1(k)} B_{1\pm}(k) \pm [1 - 2kc_{22}T(k) + 2kc_{22}T(\xi_1 k)] \times c_{11}c_{21}k \int_0^1 B_{2\pm}(k')\, e^{-d/k'} \frac{k' X(-k')}{k+k'} dk'$$

$$0 \leqslant k \leqslant 1/\xi_1 \quad (14b)$$

$$[\varphi_2^{(2)}, \mathbf{f}] = D_\pm''' + \frac{\gamma(k)}{g_2(k)} B_{2\pm}(k) \pm c_{22}k \int_0^1 B_2{}^{\pm}(k')\, e^{-d/k'} \frac{k' X(-k')}{k+k'} dk'$$

$$1/\xi_1 \leqslant k \leqslant 1 \quad (14c)$$

where

$$D'_+ = D''_+ = D'''_+ = 0 \tag{15a}$$

$$D'_- = 2A_- k(w_2 + \xi_1^2 w_1) \tag{15b}$$

$$D''_- = 2A_- c_{11}\xi_1 k[1 - 2kc_{22}T(k) + 2kc_{22}T(\xi_1 k)] \tag{15c}$$

$$D'''_- = 2A_- k w_2 \tag{15d}$$

$$[g_1(k)]^{-1} = [1 - 2kc_{11}T(\xi_1 k) - 2kc_{22}T(k)]^2 + \pi^2 k^2 (c_{11} + c_{22})^2 \tag{16a}$$

$$[g_2(k)]^{-1} = \{1 - 2kc_{11}T[1/(\xi_1 k)] - 2kc_{22}T(k)\}^2 + \pi^2 k^2 c_{22}^2. \tag{16b}$$

These equations are identical in structure to, but somewhat more complicated than, those encountered in the grey case [1].

For simplicity, we consider only the case of black plates. Then $\mathbf{f}(\mu)$ becomes

$$\mathbf{f}(\mu) = \mathbf{f} = \begin{pmatrix} w_1 \\ w_2 \end{pmatrix} \frac{\tilde{\sigma}}{\pi} T_w^4 = \boldsymbol{\psi}_+ \frac{\tilde{\sigma}}{\pi} T_w^4 \tag{17}$$

where $\tilde{\sigma}$ is the Stefan–Boltzmann constant. In this case, the left-hand sides of equations (14) all become zero and $[\boldsymbol{\psi}_+, \mathbf{f}] = N_+$.

The temperature distribution and heat transfer through the gas are given by:

$$\frac{\sigma}{\pi} T^4(x) = \frac{1}{N_+}\left[\xi_1 \int_{-1}^{1} I_1(x, \mu)\, d\mu + \int_{-1}^{1} I_2(x, \mu)\, d\mu\right] \tag{18a}$$

$$q = 2\pi \int_{-1}^{1} \mu \boldsymbol{\psi}_+(x, \mu) \cdot \mathbf{I}(x, \mu)\, d\mu = -\frac{4\pi}{3}\left(\frac{w_1}{\xi_1} + w_2\right) A_-. \tag{18b}$$

For d = 0, equation (13) leads to

$$A_- = -\frac{3\xi_1 \sigma T_w^4}{4\pi(w_1 + \xi_1 w_2)} \tag{19a}$$

so that for this case

$$q = \tilde{\sigma} T_w^4 \tag{19b}$$

as expected.

As in the grey case, the Fredholm equations may be solved by iteration. The solution converges rapidly for large plate separation but not as rapidly as in the grey case [1]. It is of interest to note that in the first approximation, in which all of the $B_{j\pm}(k)$ [or $\alpha_j(k)$] are set equal to zero, one obtains a result identical with the first approximation of the grey case (essentially, a modified diffusion approximation) with the opacity of the grey case replaced by the Rosseland mean and the Milne extrapolation distance replaced by its non-grey value,

$$q^{(1)} = \frac{4\pi}{3(\mathrm{d} + 2x_*)}\left(\frac{w_1}{\xi_1} + w_2\right). \tag{20}$$

This accounts, to some degree, for the accuracy of the Rosseland approximation which is demonstrated in the next section.

5. NUMERICAL RESULTS

In this section various approximations to the heat transfer and temperature distribution will be compared to exact results for a picket fence gas confined between black plates. The exact results were obtained from the integral equations (14) by an iteration scheme similar to that used in [1]. The function $X(-k)$ is evaluated by the method suggested by Shure and Natelson [13] that was used in the grey problem [1].

In the notation introduced earlier, the Planck (σ_p) and Rosseland (σ_r) means are:

$$\xi_p = \frac{\sigma_p}{\sigma_2} = \xi_1 w_1 + w_2 \tag{21a}$$

$$\frac{1}{\xi_r} = \frac{\sigma_2}{\sigma_r} = \frac{w_1}{\xi_1} + w_2 \tag{21b}$$

since the w_i are independent of x. The heat-transfer and temperature distributions in the Planck or Rosseland approximation (designated by $q_G(\xi_p d)$, $T_G(y, \xi_p d)$, $q_G(\xi_r d)$, and $T_G(y, \xi_r d)$, respectively) were taken to be those for a grey slab of thickness $\xi_p d$ or $\xi_r d$†. The first approximation of the iteration scheme mentioned earlier is equivalent to the Rosseland approximation (as defined here).

Another approximate method was also investigated. In this approximation, it is assumed that the radiation in the two "groups" is not coupled; that is, radiation absorbed in one of the two frequency intervals is not emitted in the other interval. The problem is then reduced to two independent "grey" problems each with its own absorption coefficient. While the assumption of decoupling is certainly not valid, this approximation is correct when $w_1 = 0$ or 1 (or when $\xi_1 = 1$) and might, therefore, be expected to be reasonably good for all values of w_1. In this approximation

$$\tilde{q}(d) = w_1 q_G(\xi_1 d) + w_2 q_G(d) \qquad (22a)$$

where $q_G(d)$ is the heat transfer for a grey gas and

$$\tilde{T}^4(y) = w_1 T_G^4(y, \xi_1 d) + w_2 T_G^4(y, d) \quad (22b)$$

where $T_G^4(y, d)$ is T^4 in a grey slab of non-dimensional thickness d at position y, $(y = 2x/d)$.

Typical results for the heat transfer are given in Figs. 3, 4 and 6 and other results showing the errors in the various approximations are given in Figs. 5 and 7. It is noted that the Rosseland approximation always overestimates the heat transfer while the Planck approximation always underestimates it. This was found in all cases studied (including a number not shown) and an examination of equation (13b) shows that it is probably always true although a rigorous proof was not found.

†Although this differs from the usual practice of restricting the use of the Rosseland mean to the diffusion approximation, the difference is small compared to the effects of interest here. This also allows us to separate, at least qualitatively, the effects of using a mean absorption coefficient from the effects on the diffusion approximation.

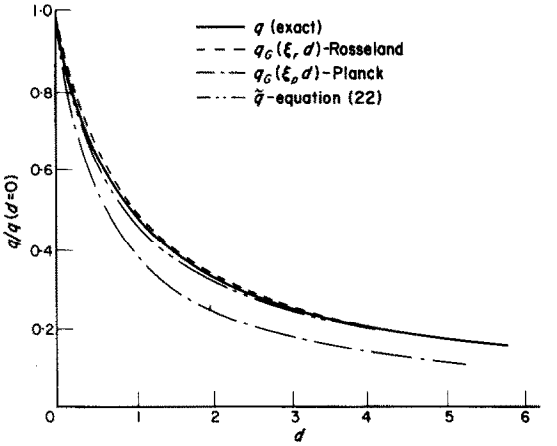

FIG. 3. Heat transfer vs. dimensionless thickness for $w_1 = 0{\cdot}25$, $\xi_1 = 5$.

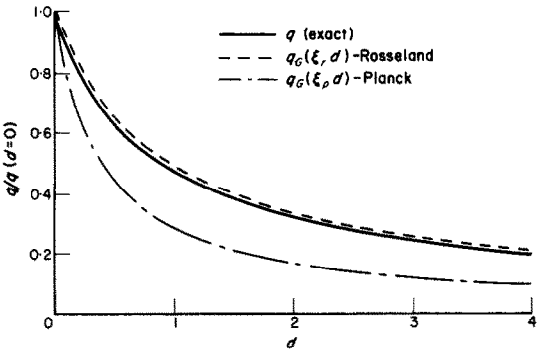

FIG. 4. Heat transfer vs. dimensionless thickness for $w_1 = 0{\cdot}25$, $\xi_1 = 10$.

The Planck approximation was shown to be very poor except for very small slab thicknesses. In fact, its use is likely to lead to significant errors whenever the gas is thicker than one mean free path with respect to the *smallest* mean free path. However, its simplicity makes it a valuable method for optically thin media.

On the other hand, the Rosseland approximation of equations (22) are fairly accurate and of roughly comparable accuracy for thick media; they also tend to bracket the exact result. Before discussing the results, we remark that the apparent improvement of the Rosseland approximation with increasing ξ_1 is to some degree, illusory. If the abscissae in Figs. 5 and 7 were thickness in Rosseland mean free paths

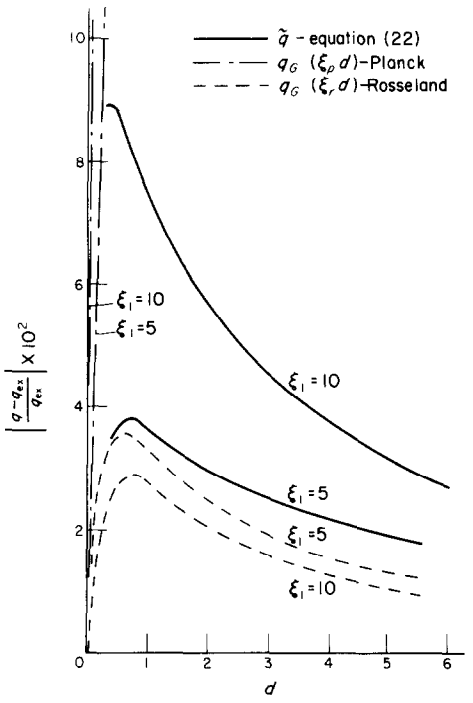

FIG. 5. Relative error in heat transfer for $w_1 = 0{\cdot}25, \xi_1 = 5, 10$.

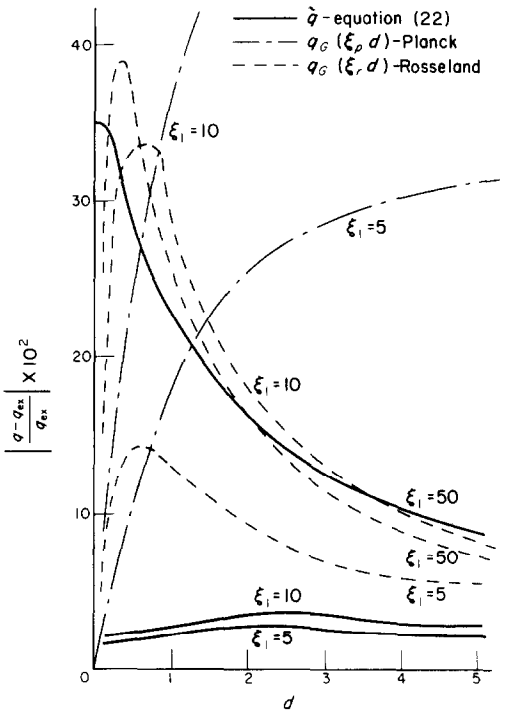

FIG. 7. Relative error in heat transfer for $w_1 = 0{\cdot}75, \xi_1 = 5, 10, 50$.

the curves with large values of ξ_1 would be stretched more than those with small values of ξ_1 and, the errors therefore, with larger ξ_1 would appear to be greater.

Comparing Figs. 5 and 7, one sees that the Rosseland approximation is more accurate for smaller values of w_1, i.e. for narrow lines. This effect can be anticipated by studying the approximations made in obtaining the Rosseland

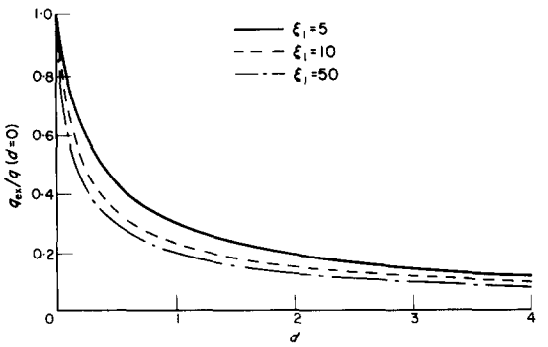

FIG. 6. Exact heat transfer vs. dimensionless thickness for $w_1 = 0{\cdot}75$.

formulae but the difference is quite striking. Qualitatively, the behaviour can be explained as follows. In the Rosseland approximation the temperature distribution is governed mainly by the band which covers the greater part of the spectrum; for large w_1, the lines dominate. Now, from the calculations for a grey gas [1], we see that, for a given gas thickness, the larger the absorption coefficient, the steeper the temperature gradient (essentially the extrapolation distance in dimensional terms becomes smaller). As a result the Rosseland approximation tends to predict too high a temperature gradient. Since the bulk of the heat flux is carried in the windows, it also tends to predict too much heat transfer and the effect is accentuated at larger line widths [14]. It should also be noted that the additional effect of using the diffusion approximation is to increase the calculated heat transfer so that the actual error in the Rosseland approximation, as usually defined, is the sum of the

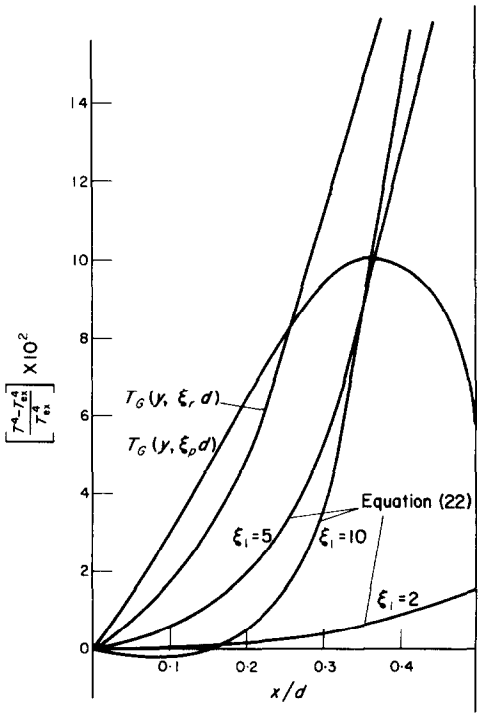

FIG. 8. Relative error in T^4 for various approximations, $w_1 = 0{\cdot}5$, $\xi_1 = 2, 5, 10$, $d = 1$.

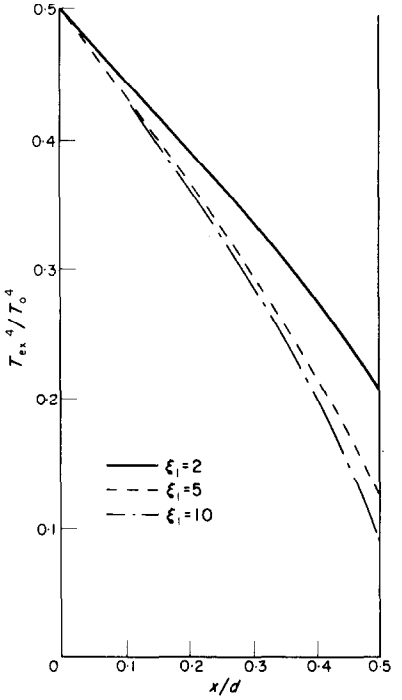

FIG. 9. Exact non-grey gas temperature vs. position for d = 1, $w_1 = 0{\cdot}5$, $\xi_1 = 2, 5, 10$.

errors shown in Figs. 5 or 7 and these corresponding to the second approximation in Fig. 3 of [1]. Thus the Rosseland approximation should be sufficiently accurate for gases with narrow lines (such as are frequently encountered in astrophysical applications) but is not as good for broad lines or bands (such as vibration–rotation bands).

Finally, in Figs. 8 and 9, the temperature distribution is considered for some typical cases. Since the temperature distributions are antisymmetric about the center line, values are given for $x/d < 0{\cdot}5$ only [15]. The error in the temperature in the Rosseland approximation, especially near the surface is greater than the error in the heat-transfer rate; the same is true for the approximation (22). The results reaffirm Stewart's conclusions [2] that non-greyness has a drastic effect on the temperature distribution near a surface. Thus no one mean absorption coefficient can transform a non-grey problem into a grey one, particularly if the temperature distribution is of interest.

It is also easy to see that in the case in which the windows are completely transparent ($\xi_1 \to \infty$) the Rosseland approximation is poor. In this case the intensities in the lines and windows are completely uncoupled and the approximation (22) is correct. It is then simple to compare the correct results with the Rosseland approximation and the error is quite large. Note, however, that Figs. 5 and 7 are unable to show this effect due to the fact that the abscissa (the plate separation) is non-dimensionalized with the window mean free path. Thus an increase in $\xi_1 (= \sigma_1/\sigma_2)$ in the figures corresponds to an increase in σ_1 rather than a decrease in σ_2.

REFERENCES

1. J. H. FERZIGER and G. M. SIMMONS, Application of Case's method to plane parallel radiative transfer, *Int. J. Heat Mass Transfer* **9**, 987–992 (1966).

2. J. C. STEWART, Non-grey radiative transfer, *Jnl Quantve Spectros. & Radiat. Transf.* **4**, 723–729 (1964).
3. J. C. STEWART, I. KUŠČER and N. J. MCCORMICK, Equivalence of special models in energy-dependent neutron transport and nongrey radiative transfer, *Ann. Phys.* **40**(2), 321–333 (1966).
4. C. E. SIEWERT and P. F. ZWEIFEL, An exact solution of equations of radiative transfer for local thermodynamic equilibrium in the non-grey case, picket fence approximation, *Ann. Phys.* **36**, 61–85 (1966).
5. C. E. SIEWERT and P. F. ZWEIFEL, Radiative transfer. II, *J. Math. Phys.* **7**(11), 2092–2102 (1966).
6. R. M. GOODY, *Atmospheric Radiation*, Vol. 1. Clarendon Press, Oxford (1964).
7. G. M. SIMMONS, Application of the method of singular eigenfunctions to radiative transfer between parallel plates, Ph.D. dissertation, Stanford University (1966).
8. R. GREIF, Energy transfer by radiation and conduction with variable gas properties, *Int. J. Heat Mass Transfer* **7**, 891–900 (1964).
9. S. CHANDRASEKHAR, *Stellar Structure*. Dover, New York (1954).
10. K. M. CASE, Elementary solutions of the transport equation and their application, *Ann. Phys.* **9**, 1–23 (1960).
11. N. I. MUSKHELISHVILI, *Singular Integral Equations*. Noordhoff, Groningen (1963).
12. H. G. KAPER, Note on the use of generalized functions and the Poincaré–Bertrand formula in neutron transport theory, *Nucl. Sci. Engng* **24**, 423–425 (1966).
13. F. SHURE and M. NATELSON, Anisotropic scattering in half-space transport problems, *Ann. Phys.* **26**, 274–285 (1964).
14. J. C. STEWART, private communication.
15. C. M. USISKIN and E. M. SPARROW, Thermal radiation between parallel plates separated by an absorbing–emitting non-isothermal gas, *Int. J. Heat Mass Transfer* **1**, 28–36 (1960).

Résumé—Le cas du transport par rayonnement entre plaques parallèles séparées par un gaz absorbant avec un coefficient d'absorption en "barrière de piquets" est traité par une méthode due à Siewert et Zweifel. Le problème est réduit à un ensemble d'équations intégrales à partir desquelles on obtient facilement des solutions numériques. Les résultats exacts sont comparés avec les approximations de Planck et de Rosseland en même temps qu'avec une nouvelle approximation. Les résultats indiquent que l'approximation de Rosseland est suffisamment précise pour des lignes de faible largeur, mais que sa précision diminue pour des lignes plus larges ou des bandes.

Zusammenfassung— Der Wärmeübergang durch Strahlung zwischen zwei parallelen Platten wird nach der Methode von Siewert und Zweifel behandelt. Für den Absorptionskoeffizienten des Gases zwischen den Platten wird ein "Zaunlattenmodell" angenommen. Das Problem wird auf einen Satz von Integralgleichungen zurückgeführt, von denen leicht numerische Lösungen gewonnen werden können. Genaue Ergebnisse werden mit den Näherungen nach Planck und Rosseland und mit einer neuen Näherung verglichen. Die Ergebnisse zeigen, dass die Rosseland-Näherung für kleine Bandweiten genügend genau ist, dass die Genauigkeit aber mit zunehmender Bandweite abnimmt.

Аннотация—Методом Сиуерта и Цвайфеля рассматривается лучистый теплообмен между параллельными пластинами, разделенными поглощающим газом с определенным коэффициентом поглощения. Задача сводится к численному решению системы интегральных уравнений. Точные результаты сравниваются с полученными приближенными решениями и решениями Планка и Росселанда. Результаты обнаруживают, что приближение Росселанда достаточно корректно для узкой линии спектра, однако, точность этого приближения уменьшается для более широких линий или полос спектра.